Mesa-type patterns in the one-dimensional Brusselator and their stability

T. KOLOKOLNIKOV †, T. ERNEUX † and J. WEI ‡

† *Université Libre de Bruxelles, Optique Nonlinéaire Théorique, Campuse Plaine, C.P. 231, 1050 Brussels, Belgium*
terneux@ulb.ac.be, tkolokol@ulb.ac.be
‡ *Department of Mathematics, The Chinese University of Hong Kong, Shatin, Hong Kong*
wei@math.cuhk.edu.hk

(*Draft copy as of 27 April 2005*)

The Brusselator is a generic reaction-diffusion model for a tri-molecular chemical reaction. We consider the case when the input and output reactions are slow. In this limit, we show the existence of K-periodic, spatially bi-stable structures, *mesas*, and study their stability. Using singular perturbation techniques, we find a threshold for the stability of K mesas. This threshold occurs in the regime where the exponentially small tails of the localized structures start to interact. By comparing our results with Turing analysis, we show that in the generic case, a Turing instability is followed by a slow coarsening process whereby logarithmically many mesas are annihilated before the system reaches a steady equilibrium state. We also study a "breather"-type instability of a mesa, which occurs due to a Hopf bifurcation. Full numerical simulations are shown to confirm the analytical results.

1 Introduction

In 1952, Turing proposed that the formation of spatial patterns during morphogenesis could be explained in terms of the instability of a homogeneous steady-state solution of a reaction-diffusion network describing the evolution of a set of morphogens [**31**]. Turing himself illustrated his ideas on two chemical models. Turing's original work is primarily concerned with the stability analysis of the homogeneous steady-state solution of the rate equations for the interacting morphogens [**22**]. The main point of biological interest, however, is whether stable spatial structures may be generated beyond the instability, i.e., whether the rate equations admit stable (and positive) inhomogeneous solutions exhibiting the most characteristic features of morphogenetic patterns.

This point has been taken up seriously in the early seventies. More systematic numerical studies of Turing's model have been performed showing irregular spatial structures [**4**]. This led to serious reservations about the relevance of Turing's theory in developmental biology, particularly its ability to generate regular patterns. But these criticisms originate from a somewhat unfortunate choice of Turing's example and they do not touch the essential points of Turing's theory. More specifically, the obvious requirement that the rate equations must admit positive and bounded solutions is not satisfied in Turing's example [**11**].

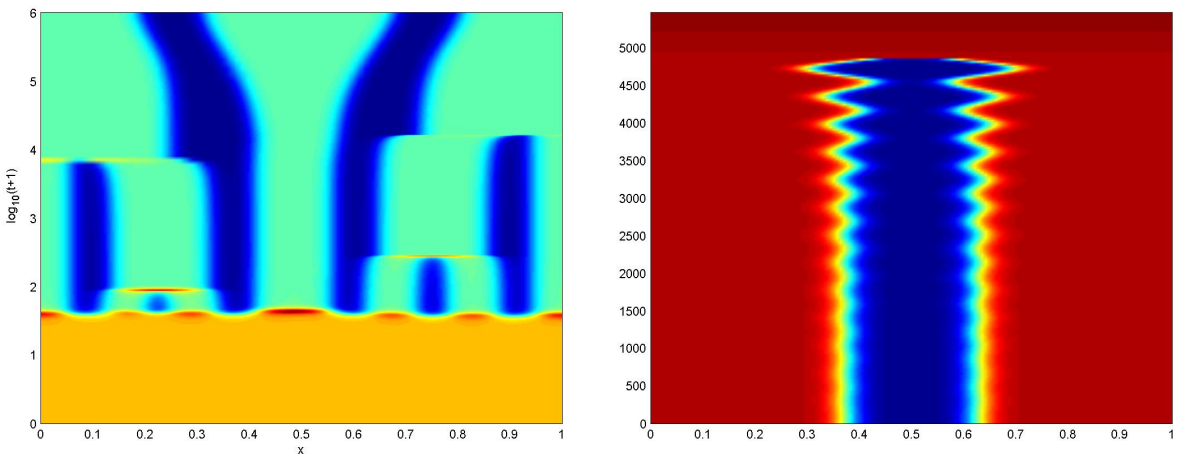

(a) (b)

FIGURE 1. (a) Turing instability and mesa-type localized structures. The parameters are $A = 1, B = 8,\ \varepsilon = 10^{-4},\ D = 10,\ \tau = 10$. Initial steady state was set to $u = A, v = A/B$, perturbed by a very small random noise. Note the logarithmic scale for time. Initial Turing instability triggers a $k = 7$ mode at time $t \sim 50$. Thereafter a coarsening process takes place until there are only two mesas left. (b) Slow-time oscillatory instability of a single spike solution to (1.1). The parameter values are $A = 1,\ B = 8,\ D = 10,\ \varepsilon = 0.00025,\ \tau = 0.999$.

Because of this misunderstanding on Turing's fundamental contribution, other two-variable models satisfying the law of mass action have been explored. In 1968, Prigogine and Lefever [**28**] introduced a two variable system that exhibits an autocatalytic reaction (called the "Brusselator"). The simplicity of the rate equations motivated analytical and numerical studies which showed the existence of stable structures [**3**]. The Brusselator is based on the following intermediate reactions for the two chemical intermediates X and Y:

$$A \to X, \quad C + X \to Y + F, \quad 2X + Y \to 3X, \quad X \to E.$$

The global reaction is $A + C \to F + E$ and corresponds to the transformation of inputs products A and C into output products F and E. We assume (without loss of generality) that the rate constants for the first and last step are equal to r whereas the intermediate rate constants are one. The rates equations then become

$$\begin{aligned} X_t &= D_x X_{xx} + rA - CX + X^2 Y - rX \\ Y_t &= D_y Y_{xx} + CX - X^2 Y. \end{aligned}$$

Since the discovery of spatial patterns in 1970's, various Turing patterns in the Brusselator were studied both numerically and analytically in one, two and three dimensions. These include spots, stripes, labyrinths and and hexagonal patterns, [**12**], [**22**], [**35**], [**30**], [**36**] oscillatory instabilities and spatio-temporal chaos [**18**], [**37**]. While Turing analysis and its weakly nonlinear extension have been successful at detecting and classifying possible pattern types, its range of applicability is limited. Indeed Turing patterns are

assumed to be small sinusoidal perturbations of a homogeneous state. In practice however, many solutions contain sharp transitions such as spikes and kinks. Such patterns are not amenable to Turing analysis since they are far away from the homogeneous state. In this paper we study *mesa*-type patterns.[1] These are box-like patterns that join two flat regions of space with sharp transition layers, such as shown in Figure 2. Such patterns are far away from the homogenous steady state.

Most analytical and numerical studies assumed that all kinetic reaction rates are the same ($r = 1$) and used the fixed concentrations A, C as control parameters. By contrast, in this paper we concentrate on the case where the first and last two steps are slow in comparison to the intermediate steps, so that r is small.

For our analysis it will be convenient to use the following scaling,

$$\begin{aligned} \tau u_t &= D\varepsilon u_{xx} + \varepsilon A - Bu + u^2 v - \varepsilon u \\ v_t &= D\varepsilon v_{xx} + Bu - u^2 v \end{aligned} \tag{1.1}$$

where

$$\tau = \frac{D_y}{D_x}, \quad \varepsilon = r\frac{D_y}{D_x}, \quad B = C\frac{D_y}{D_x}, \quad D = \frac{D_x}{r},$$
$$u = X, \qquad v = \tau Y$$

and the spatial domain is $x \in [0, 1]$ with the zero flux boundary conditions

$$u_x = 0 = v_x \quad \text{at } x = 0 \text{ and } 1.$$

In this work we assume the following conditions,

$$r \ll D_x \leq O(D_y) \ll 1, \qquad A = O(1), \quad C = O\left(\frac{D_x}{D_y}\right). \tag{1.2}$$

In particular this implies that the the input and output reactions are slow compared to the intermediate steps. In terms of our scaling we have

$$\varepsilon D \ll 1, \quad D \gg 1; \qquad O(A) = 1 = O(B), \tag{1.3}$$

$$O(\tau) \geq 1. \tag{1.4}$$

As a motivation, let us present two numerical examples. On Figure 1.a we show a typical time evolution on a very long time interval. The homogeneous steady state is unstable because of Turing instability but the expected Turing sinusoidal pattern only appears after a delay ($t > 50$). Turing's structure then gradually deteriorates and relatively quickly moves into a new pattern formed by several localized mesa-type structures. They then undergo a coarsening process over a logarthmically long time-scale and, eventually, only two mesas remain. Turing's analysis can be used to predict the first pattern ($t \sim 50$) but it cannot anticipate the coarsening process or the number of final mesas. As we shall demonstrate, in the case $B > A^2$, the Turing pattern is characterized by a wave number proportional to $k = O\left(\frac{1}{\sqrt{D\varepsilon}}\right)$ while the number of stable long-time mesas has the order

[1] Mesa means table in Spanish; it is also a name given to square boulders which are found in the Colorado desert. The use of this term was suggested by Fife [**13**].

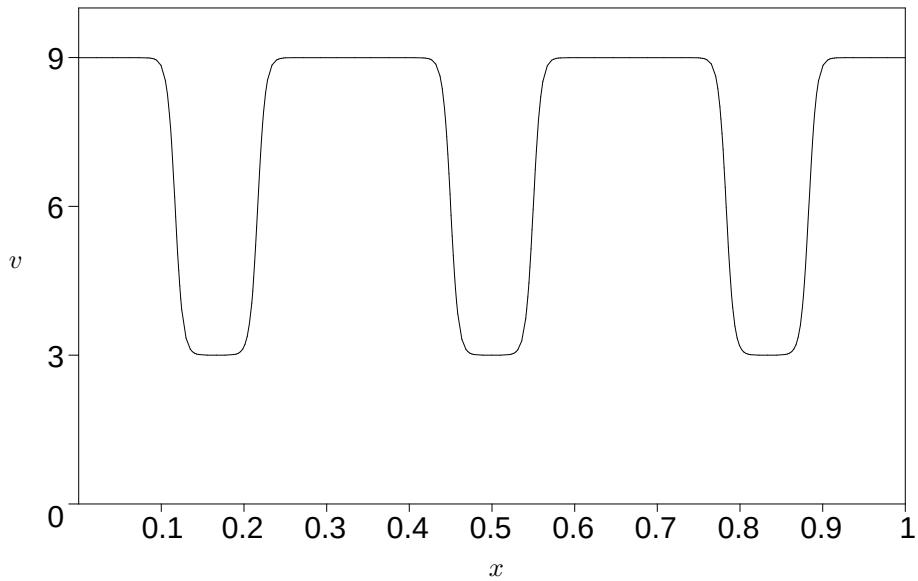

FIGURE 2. An example of a three-mesa equilibrium solution for v. Here, $K = 3,\ A = 2,\ B = 18,\ \varepsilon D = 0.02^2$, $w_0 = 9$, $l = 0.11$.

$K = O\left(\frac{1}{\sqrt{D\varepsilon}\ln\frac{1}{\varepsilon}}\right)$, so that k is logarithmically bigger than K. This is the underlying cause of the coarsening process observed in Figure 1.a.

In the second experiment shown in Figure 1.b, a single mesa undergoes a "breather"-type oscillatory instability which eventually leads to its extinction. Both coarsening and the breather instability occur at a slow timescale. The main goal of this work is to describe these instabilities analytically.

Our results are related to the study of bistable systems, see for example [**29**], [**15**], [**23**] [**24**], [**25**], [**26**], [**27**], [**8**]. Mesa patterns also appear in the FitzHugh-Nagumo model [**15**], certain phase separation models such as Cahn-Hilliard, Allen-Cahn, [**1**], [**2**], [**6**] and block-copolymers [**29**]. For these systems the resulting spectral problem has small eigenvalues, also called critical spectra, that tend to zero with the thickness of the interfaces. Typically k such layers are stable [**26**]. However as we show in this paper, if the number of layers is excessively large, instabilities can occur. This happens when the exponentially small interaction outside the interface locations cannot be ignored. Our main new contribution is to study this interaction, and to show that it has a destabilizing effect.

1.1 Summary of main results

We now summarize our main results. We first describe the shape of the equilibrium K mesa solutions. In Section 2 we show the following.

Proposition 1 *Consider the equilibrium-state problem,*

$$0 = \varepsilon D v_{xx} + Bu - u^2 v, \qquad 0 = \varepsilon D u_{xx} + \varepsilon A + u^2 v - (B+\varepsilon)\, u, \qquad x \in [0,1]\,,$$
$$u' = 0 = \ v' \quad \text{at} \quad x = 0 \text{ or } x = 1.$$

in the limit (1.3) and suppose that

$$A^2 < 2B. \tag{1.5}$$

Then there exists a K-mesa symmetric solution to (v,u) of the following form.

Let

$$w_0 = 3\sqrt{B/2}, \qquad l = \frac{A}{K\sqrt{2B}}, \qquad d = \frac{1}{K} - l, \tag{1.6}$$

$$x_{li} \equiv x_i - \frac{l}{2}, \quad x_{ri} \equiv x_i + \frac{l}{2}, \quad x_i \equiv \frac{\left(\frac{1}{2}+i\right)}{K}, \qquad i = 1 \ldots K. \tag{1.7}$$

For x away from x_{ri}, x_{li}, we have:

$$v \sim \begin{cases} w_0, & x \in [0,1] \backslash \cup\, [x_{li}, x_{ri}] \\ \frac{w_0}{3}, & x \in \cup\, (x_{li}, x_{ri}) \end{cases}$$

For x near the interfaces x_{ri}, x_{li} we have,

$$v \sim \begin{cases} v_l(x - x_{li}), & x - x_{li} \le O(\sqrt{\frac{\varepsilon D}{B}}) \\ v_r(x - x_{ri}), & x - x_{ri} \le O(\sqrt{\frac{\varepsilon D}{B}}) \end{cases}$$

where

$$v_r = w_0 \frac{2}{3} + w_0 \frac{1}{3} \tanh\left(\frac{w_0}{3} \frac{x}{\sqrt{2\varepsilon D}}\right), \qquad v_l = w_0 \frac{2}{3} - w_0 \frac{1}{3} \tanh\left(\frac{w_0}{3} \frac{x}{\sqrt{2\varepsilon D}}\right).$$

Finally,

$$u \sim w_0 - v.$$

A typical such solution with $K = 3$ is illustrated on Figure 2.

We next analyse the stability of such equilibrium. There are two distinguished limits of interest, either $DK^2 \ll O\left(\frac{1}{\varepsilon \ln^2 \varepsilon}\right)$ or $DK^2 = O\left(\frac{1}{\varepsilon \ln^2 \varepsilon}\right)$. The former is studied in Sections 3 and 4 while the latter in Section 5. In Section 3 we derive rather precise results for eigenvalues, summarized in the following theorem.

Theorem 2 *Consider a K mesa solution of Proposition 1. Suppose in addition that*

$$1 \ll DK^2 \ll O\left(\frac{1}{\varepsilon \ln^2 \varepsilon}\right) \qquad \text{and} \quad O\left(\tau - 1\right) \gg 0.$$

Such solution is stable when $\tau - 1 \gg 0$ and unstable when $\tau - 1 \ll 0$. There are $2K$ small eigenvalues of order $O\left(\varepsilon\right)$; all other eigenvalues are negative and have order $\ge O\left(D\varepsilon\right)$.

The smallest $2K$ eigenvalues are given by

$$\lambda_{j\pm} \sim \frac{-1 \pm \sqrt{1 - 2K^2 dl\left[1 - \cos\left(\frac{\pi j}{K}\right)\right]}}{2(\tau - 1)}\varepsilon, \qquad j = 1 \ldots K-1;$$
$$\lambda_- \sim \frac{-Kl}{\tau - 1}\varepsilon, \qquad \lambda_+ = \frac{-1}{\tau - 1}\varepsilon.$$

and are all negative when $\tau > 1$, and positive when $\tau < 1$. The transition from stability to instability occurs via a Hopf bifurcation as τ is decreased past τ_h where to leading order, $\tau_h \sim 1$.

Note that near the interfaces, the gradient changes on the order $\delta = \sqrt{\varepsilon D}$. In terms of δ, the scaling $DK^2 = O(\frac{1}{\varepsilon \ln^2 \varepsilon})$ can be written as

$$D = O\left(\delta^2 \exp\left(\frac{1}{K\delta}\right)\right).$$

Thus Theorem 2 confirms the stability of K mesas when $\tau > 1$ as long as D is not exponentially large in δ. In the contrary case, we derive the following result in Section 5.

Theorem 3 *Suppose that*

$$\tau > 1$$

and let

$$D_K = \frac{1}{K^2} D_1 \quad \textit{where} \quad D_1 \sim \begin{cases} \dfrac{A^2}{2\varepsilon \ln^2\left(\frac{12\sqrt{2}AB^{3/2}}{\varepsilon(\sqrt{2B}-A)^2}\right)}, & 2A^2 < B \\ \dfrac{\left(\sqrt{2B}-A\right)^2}{2\varepsilon \ln^2\left(\frac{12\sqrt{2}}{\varepsilon A}B^{3/2}\right)}, & 2A^2 > B \end{cases} + l.s.t.$$

Here, l.s.t. denotes logarithmically small terms. Then a K mesa symmetric equilibrium with $K \geq 2$ is stable if $D < D_K$ and is unstable otherwise. Moreover, a single-mesa equilibria $K = 1$ is always stable. A more precise value for D_1 is given in Proposition 8.

Theorem 3 states that the instability threshold occurs when D is exponentially large. In this case the exponentially fast decay outside the interface locations must be taken into account. Their exponentially weak interaction is responsible for an eventual loss of stability. Figure 3 illustrates this proposition. Indeed using the parameters used in that simulation we deduce from Proposition 8 that $D_1 = 20.96$; so that $D_2 = 5.28$. Since $D = 10 > D_2$, the two-mesa equilibrium state is unstable.

Our next result is about the presence of a Hopf bifurcation when τ is near 1.

Theorem 4 *Suppose that*

$$\sqrt{\frac{B}{\varepsilon D}} \ll DK^2 \ll O\left(\frac{1}{\varepsilon \ln^2 \varepsilon}\right). \tag{1.8}$$

Let

$$\tau_{h_+} = 1 + \frac{1}{4D}\left(ld - \frac{K}{3}\left(d^3 + l^3\right)\right) \tag{1.9}$$

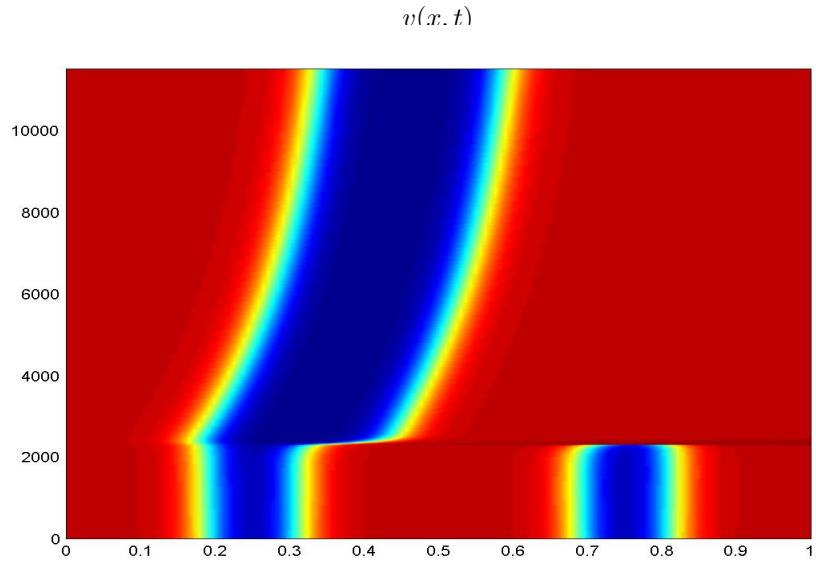

FIGURE 3. Slow-time competition instability of a two-mesa solution to (1.1). The parameter values are $A = 1,\ B = 8,\ D = 10,\ \varepsilon = 0.00025,\ \tau = 1.3$

where K, d, l are as in Proposition 1. Then a K-mesa solution undergoes a Hopf bifurcation when $\tau = \tau_{h_+}$. It is stable when $\tau > \tau_{h_+}$ and unstable otherwise. When $\tau = \tau_{h_+}$, the corresponding eigenvalue has value

$$\lambda_+ \sim i\sqrt{8K}\left(\varepsilon^3 DB\right)^{1/4}$$

Figure 1.b illustrates the type of oscillations that occur when $\tau < \tau_{h+}$. Theorem 4 is able to predict the onset of such oscillations even though it says nothing about whether this bifurcation is supercritical or subcritical.

Finally we perform a Turing stability analysis of the Brusselator in Section 6. We find that in the generic case, the modes k within the Turing instability band have the order $O(\frac{1}{\delta})$ where $\delta = \sqrt{\varepsilon D}$ is the width of the interface. On the other hand the mesa instability threshold occurs when $K = O\left(\frac{1}{\delta \ln \frac{1}{\varepsilon}}\right)$. It is then clear that $k \gg K$ by a logarithmically large amount. This is the underlying reason for the coarsening process observed in Figure 1.a.

One of the easy consequences of Turing's analysis is the existence of the regime for which mesa-type structures are stable at the same time as the homogeneous steady state. A more interesting question is the following.

Open problem 5 *Does there exist a parameter regime for which the mesa-type solution is unstable, and in addition the homogeneous steady state $u = A,\ v = \frac{B}{A}$ is unstable with respect to the Turing instability?*

An existence of such a regime would imply spatio-temporal chaos in the Brusselator. We answer this question in the negative for the case when

$$\frac{1}{\delta} \ll D \ll \delta \exp\left(\frac{1}{\delta}\right), \qquad \delta = \sqrt{\varepsilon D}.$$

2 Steady state

In this section we derive the asymptotics of the steady-state solution to the Brusselator (1.1). Let

$$w = v + u. \tag{2.1}$$

Then we obtain

$$v_t = \delta^2 v_{xx} + B\left(w - v\right) - \left(w - v\right)^2 v, \tag{2.2}$$

$$\frac{1}{\varepsilon}\left(v_t + \tau\left(w_t - v_t\right)\right) = D w_{xx} - w + v + A \tag{2.3}$$

where

$$\delta^2 = \varepsilon D.$$

The steady-state equations then become

$$\begin{cases} 0 = \delta^2 v_{xx} + B\left(w - v\right) - \left(w - v\right)^2 v, \\ 0 = D w_{xx} - w + v + A \end{cases}, x \in [0, L]$$

$$v_x(0) = 0 = v_x(L), \qquad w_x(0) = 0 = w_x(L).$$

Next we expand in $\frac{1}{D}$,

$$v = v_0 + \frac{1}{D} v_1 + \ldots,$$
$$w = w_0 + \frac{1}{D} w_1 + \ldots$$

We obtain $w_0'' = 0$ so that Then w_0 is a constant to be determined. For v_0 we obtain

$$\delta^2 v_{0xx} = F(w_0, v_0)$$

where

$$F(v, w) \equiv B\left(v - w\right) + \left(v - w\right)^2 v.$$

We seek solutions for w_0 such that $F(w_0, v)$ is a cubic in v_0 with equidistant roots. This is the so-called Maxwell line condition, and implies that the integral of F between its first two roots is the negative of the integral between the last two. When this is the case, the solution for v_0 will be a kink-like solution in the form of a tanh. An example of such solution is shown on Figure 2. The condition of equidistant roots is equivalent to solving two equations

$$F_{vv}(v, w) = 0 = \ F(v, w)$$

for unknowns B and w. A simple computation shows that this is equivalent to

$$B = \frac{2}{9} w_0^2. \tag{2.4}$$

Substituting for B we obtain

$$F(v_0,w_0) = (v_0 - w_0)^2 v_0 - \frac{2}{9} w_0^2 (v_0 - w_0) = \left(v_0 - \frac{1}{3} w_0\right)\left(v_0 - \frac{2}{3} w_0\right)(v_0 - w_0) \quad (2.5)$$

On the entire space, the ODE $\delta^2 v_0'' = F(v_0, w_0)$ with F as in 2.5 admits the following two solutions,

$$v_r = w_0 \frac{2}{3} + w_0 \frac{1}{3} \tanh\left(\frac{w_0}{3} \frac{x}{\sqrt{2}\delta}\right), \quad (2.6)$$

$$v_l = w_0 \frac{2}{3} - w_0 \frac{1}{3} \tanh\left(\frac{w_0}{3} \frac{x}{\sqrt{2}\delta}\right). \quad (2.7)$$

We are interested in mesa-type solutions. A single, symmetric mesa-type solution on an interval $[0, L]$ has the form,

$$v_0 \sim \begin{cases} v_l (x - x_l), & x < \frac{L}{2} \\ v_r (x - x_r), & x > \frac{L}{2} \end{cases}.$$

Here, we chose

$$x_l = \frac{L - l}{2}, \qquad x_r = \frac{L + l}{2}.$$

where l is the width of the mesa to be determined. A K-spike symmetric solution on the interval $[0, 1]$ is then obtained by glueing together K solutions on the interval $L = \frac{1}{K}$. Such a solution has $2K$ interfaces whose locations are given by x_{li}, x_{ri} defined in (1.7). To find l we need the second order equations. We have,

$$\delta^2 v_{1xx} = F_v(v_0,w_0) v_1 + F_w(v_0,w_0) w_1, \quad (2.8)$$

$$w_{1xx} = w_0 - v_0 - A \quad (2.9)$$

where

$$F_v(v, w) = B + (v - w)(3v - w), \quad F_w(v, w) = -B + 2(w - v) v.$$

Using the boundary condition $w_1'(\pm L) = 0$ we obtain

$$\int_0^L (w_0 - v_0 - A) = 0.$$

We evaluate

$$\int_0^L v_0 \sim l \frac{w_0}{3} + w_0 (L - l)$$

from where

$$l \sim \frac{3}{2} \frac{LA}{w_0} \sim \frac{LA}{\sqrt{2B}}. \quad (2.10)$$

Substituting $L = \frac{1}{K}$ then yields Proposition 1.

We remark that the equation (2.9) for w_1 with Neumann boundary condition is solvable up to a constant. See Section 5, Lemma 9 for the determination of this constant.

3 Stability in the regime $DK^2 \ll O\left(\frac{1}{\varepsilon}\ln^2\varepsilon\right)$

In this section we derive Theorem 2, valid when $D \ll O\left(\frac{1}{\varepsilon\ln^2\varepsilon}\right)$. Before showing this result, we derive a more general formula for eigenvalues which is valid for all τ. We show the following.

Lemma 6 *Consider a K-mesa symmetric equilibrium solution as given in Proposition 1. Moreover suppose that*

$$1 \ll DK^2 \ll O\left(\frac{1}{\varepsilon}\ln^2\varepsilon\right).$$

The eigenvalues of such equilibrium state are asymptotically given implicitly by

$$\lambda \sim 2\sqrt{B\frac{\varepsilon}{D}}\left(ldK - \frac{2}{\sigma}\frac{(\tau-1)\lambda+\varepsilon}{\varepsilon}\right) \tag{3.1}$$

where σ may take one of the following $2K$ values

$$\sigma_{j\pm} = \left(c \pm \sqrt{a^2+b^2+2ab\cos(\theta)}\right), \quad \theta = \frac{\pi j}{K}, \quad j = 1\ldots K-1$$
$$\sigma_{\pm} = c + a \pm b$$

where

$$a = \frac{-\mu_d}{\sinh(\mu_d d)}, \qquad b = \frac{-\mu_l}{\sinh(\mu_l l)}, \qquad c = \mu_d\coth(\mu_d d) + \mu_l\coth(\mu_l l),$$

$$\mu_l \equiv \frac{\sqrt{2\varepsilon+\lambda(2\tau-1)}}{\delta}, \qquad \mu_d \equiv \frac{\sqrt{\lambda}}{\delta}. \tag{3.2}$$

Proof. We start by linearizing around the equilibrium solution (v, w). We write,

$$v(x,t) = v(x) + e^{\lambda t}\phi(x), \quad w(x,t) = w(x) + e^{\lambda t}\psi(x)$$

where we assume that ψ and ϕ are small. We obtain

$$\lambda\phi = \delta^2\phi_{xx} - F_v(v,w)\phi - F_w(v,w)\psi, \tag{3.3 a}$$

$$\frac{1}{\varepsilon}(\phi + \tau(\psi-\phi))\lambda = D\psi_{xx} - \psi + \phi \tag{3.3 b}$$

where $\delta = \sqrt{\varepsilon D}$. Using (2.4) we obtain

$$F_v(v_0,w_0) = 3v_0^2 - 4w_0v_0 + \left(w_0^2+B\right) = 3v_0^2 - 4w_0v_0 + \frac{11}{9}w_0^2,$$
$$F_w(v_0,w_0) = -2v_0^2 + 2w_0v_0 - B = -2v_0^2 + 2w_0v_0 - \frac{2}{9}w_0^2.$$

so that

$$F_v(w_0,w_0) = B, \quad F_w(w_0,w_0) = -B$$
$$F_v(\frac{w_0}{3},w_0) = B, \quad F_w(\frac{w_0}{3},w_0) = B$$

Note that away from kink locations x_{li}, x_{ri}, the diffusion term $\varepsilon D\phi''$ may be neglected and we have $\phi \sim -\frac{F_w(v_0,w_0)}{F_v(v_0,w_0)}\psi$. On the other hand, near the kink locations we locally

estimate the eigenfunction by the derivative of the profile. This suggests the following asymptotic form:

$$\phi \sim \begin{cases} c_{li} v'_{li}, & x \sim x_{li} \\ c_{ri} v'_{ri}, & x \sim x_{ri} \\ \psi, & x \notin (x_{li}, x_{ri}), \quad i = 1 \dots K \\ -\psi, & x \in (x_{li}, x_{ri}), \quad i = 1 \dots K \end{cases}.$$

where the constants c_{li} and c_{ri} are to be found. We multiply (3.3 *a*) by v'_{li} and integrate. Because of exponential decay, we obtain that $\int v'_{li}\phi \sim c_{li} \int v'^2_{li}$. Therefore

$$\lambda \int v'^2_{li} + \int v'_{li} F_w(v_{li}, w_0)\psi \sim \int \left[\delta^2 v'_{li}\phi_{xx} - v'_{li}\phi F_v(v_{li}, w_0) - v'_{li}\phi \frac{1}{D} \left(F_{vv}(v_{li}, w_0) v_1 + F_{vw}(v_{li}, w_0) w_1 \right) \right].$$

Using integration by parts we obtain,

$$\int \left[\varepsilon D v'_{li}\phi_{xx} - v'_{li}\phi F_v(v_{li}, w_0) \right] \sim 0.$$

Next we evaluate

$$I = \int v'_{li}\phi \left(F_{vv}(v_{li}, w_0) v_1 + F_{vw}(v_{li}, w_0) w_1 \right).$$

Differentiating (2.8) we have

$$\delta^2 v''_1 - v'_l \left(F_{vv}(v_{li}, w_0) v_1 + F_{vw}(v_{li}, w_0) w_1 \right) - F_v(v_{li}, w_0) v'_1 - F_w(v_{li}, w_0) w'_1 = 0$$

so that

$$\begin{aligned} I &= \int \phi \left(\delta^2 v''_1 - F_v(v_{li}, w_0) v'_1 - F_w(v_{li}, w_0) w'_1 \right) \\ &\sim - \int c_{li} v'_l F_w(v_{li}, w_0) w'_1 \end{aligned}$$

Therefore we obtain

$$c_{li}\lambda \int_{x_{li}^-}^{x_{li}^+} v'^2_{li} + \psi(x_{li}) \int_{x_{li}^-}^{x_{li}^+} v'_{li} F_w(v_0, w_0) \sim c_{li} w'_1(x_{li}) \int_{x_{li}^-}^{x_{li}^+} v'_{li} F_w(v_0, w_0),$$

Here and below, the symbol $\int_{x_{li}^-}^{x_{li}^+}$ denotes integration over the interface located at x_{li}. Since v'_0 decays exponentially outside the interface, this symbol is unambigious; that is $\int_{x_{li}^-}^{x_{li}^+} = \int_0^1 + e.s.t.$ Next we show,

$$\int_{x_{li}^-}^{x_{li}^+} v'_{li} F_w(v_0, w_0) \sim -\frac{8}{81} w_0^3, \qquad \int_{x_{li}^-}^{x_{li}^+} v'^2_{li} \sim \frac{2\sqrt{2} w_0^3}{81\delta}.$$

We have $\int_{x_l^-}^{x_l^+} v'_{li} F_w(v_0, w_0) = G(v(x_{li}^+)) - G(v(x_{li}^-))$ where $G(v) \equiv \int F_w(v, w_0) dv = -\frac{2}{3}v^3 + w_0 v^2 - \frac{2}{9} w_0^2 v$. We have $v(x_{li}^+) = w/3,\ v(x_{li}^-) = w_0$ so that $G(v(x_{li}^+)) - G(v(x_{li}^-)) = \left[\frac{1}{81} - \frac{1}{9} \right] w_0^3 = -\frac{8}{81} w_0^3$.

To evaluate the second integral, use the explicit formula (2.7) for v_l and the fact that $\int_{-\infty}^{+\infty} \operatorname{sech}^4(y)\, dy = \frac{4}{3}$.

Using (2.9) and (2.10) yields

$$w_1'(x_{li}) \sim -\frac{w_0 l d K}{3D}.$$

Therefore we obtain

$$c_{li}\lambda\frac{\sqrt{2}}{\delta} = 4\left(c_{li}\left(\frac{1}{3}\frac{ldK}{D}w_0\right) + \psi(x_{li})\right), \tag{3.4}$$

An analogous computation yields

$$-c_{ri}\lambda\frac{\sqrt{2}}{\delta} = 4\left(-c_{ri}\left(\frac{1}{3}\frac{ldK}{D}w_0\right) + \psi(x_{ri})\right), \tag{3.5}$$

It remains to compute $\psi(x_{li})$. Inside the intervals (x_{li}, x_{ri}) we have $\phi \sim -\psi$ and outside those intervals we have $\phi \sim \psi$. In addition we assume that near kinks, ψ changes much slower than ϕ. In this case we may replace

$$v_{li}' \sim -\frac{2}{3}w_0\boldsymbol{\delta}(x - x_{li}), \quad v_{ri}' \sim \frac{2}{3}w_0\boldsymbol{\delta}(x - x_{ri}).$$

inside the equation (3.3 b). Here and below, $\boldsymbol{\delta}$ denotes the Dirac delta function. Therefore we obtain,

$$\psi_{xx} - \mu^2\psi \sim -\alpha\sum_{i=1}^{K} c_{li}\boldsymbol{\delta}(x - x_{li}) - c_{ri}\boldsymbol{\delta}(x - x_{ri})$$

where

$$\mu \sim \mu_l \equiv \frac{\sqrt{2\varepsilon + \lambda(2\tau - 1)}}{\delta}, \quad x \in (x_{li}, x_{ri})$$
$$\mu \sim \mu_d \equiv \frac{\sqrt{\lambda}}{\delta}, \quad x \notin (x_{li}, x_{ri}).$$

and

$$\alpha = \frac{2}{3}w_0\frac{(1-\tau)\lambda - \varepsilon}{\delta^2}.$$

Next we apply the following lemma.

Lemma 7 *Suppose that*

$$u'' - \mu^2 u = -\left(\sum b_{li}\boldsymbol{\delta}(x - x_{li}) + b_{ri}\boldsymbol{\delta}(x - x_{ri})\right) \tag{3.6}$$

$$\textit{with} \quad u'(0) = 0 = u'(1) \tag{3.7}$$

where x_{li}, x_{ri} are given in (1.7) and

$$\mu = \begin{cases} \mu_l & x \in (x_{li}, x_{ri}) \\ \mu_d & x \notin (x_{li}, x_{ri}) \end{cases}.$$

Let

$$\vec{u} \equiv \begin{bmatrix} u\left(x_{l1}\right) \\ u\left(x_{r1}\right) \\ \vdots \\ u\left(x_{lK}\right) \\ u\left(x_{rK}\right) \end{bmatrix}, \qquad \vec{b} \equiv \begin{bmatrix} b_{l1} \\ b_{r1} \\ \vdots \\ b_{lK} \\ b_{rK} \end{bmatrix}.$$

Then

$$\vec{u} = \mathbf{M}\vec{b}$$

where

$$M^{-1} = \begin{bmatrix} a+c & b & & & & & \\ b & c & a & & & & \\ & a & c & b & & & \\ & & & \cdots & & & \\ & & & & a & c & b \\ & & & & & b & c+a \end{bmatrix}$$

with

$$a = \frac{-\mu_d}{\sinh\left(\mu_d d\right)}, \qquad b = \frac{-\mu_l}{\sinh\left(\mu_l l\right)}, \qquad c = \mu_d \coth\left(\mu_d d\right) + \mu_l \coth\left(\mu_l l\right).$$

The eigenvalues σ of $\mathbf{M}^{-1}$ are given as follows

$$\sigma_{j\pm} = \left(c \pm \sqrt{a^2 + b^2 + 2ab\cos\left(\theta\right)}\right), \quad \theta = \frac{\pi j}{K}, \quad j = 1 \ldots K-1$$
$$\sigma_{\pm} = c + a \pm b.$$

The two eigenvalues $\sigma_{\pm}$ may be written explicitly as

$$\sigma_{+} = \mu_d \tanh\left(\mu_d d/2\right) + \mu_l \tanh\left(\mu_l l/2\right),$$
$$\sigma_{-} = \mu_d \tanh\left(\mu_d d/2\right) + \mu_l \coth\left(\mu_l l/2\right).$$

This lemma was derived in [**29**]; for convenience of the reader we give its proof in Appendix A.

Define

$$\vec{\psi} = \begin{bmatrix} \psi\left(x_{l1}\right) \\ \psi\left(x_{r1}\right) \\ \vdots \\ \psi\left(x_{lK}\right) \\ \psi\left(x_{rK}\right) \end{bmatrix}, \qquad \vec{d} = \begin{bmatrix} c_{l1} \\ -c_{r1} \\ \vdots \\ c_{lK} \\ -c_{rK} \end{bmatrix}$$

Using Lemma 7 we have,

$$\vec{\psi} = \alpha \mathbf{M}\vec{d}$$

and we write (3.4, 3.5) as

$$\vec{d}\lambda\sqrt{\frac{2}{\varepsilon D}}. = 4\left(\vec{d}\left(\frac{1}{3}\frac{ldK}{D}w\right) + \alpha\mathbf{M}\vec{d}\right).$$

Therefore we have

$$\lambda_j\sqrt{\frac{2}{\varepsilon D}} = 4\left(\frac{1}{3}\frac{ldK}{D}w + \alpha\sigma^{-1}\right), \quad j = 1\ldots 2K \tag{3.8}$$

where σ are $2K$ eigenvalues of $\mathbf{M}^{-1}$.

This completes the proof of Lemma 6. ■

We now come back to the proof of Theorem 2. Assuming $O(\tau-1) \gg 0$, the dimensional analysis shows that two scalings are possible, either $\lambda = O(\varepsilon)$ or $\lambda = O(D\varepsilon)$.

We first consider the case

$$\lambda = \varepsilon\lambda_0.$$

Using the notation of Lemma 6 we then obtain

$$\mu_d^2 = \frac{\lambda_0}{D} \ll 1, \quad \mu_l^2 = \frac{2+\lambda_0\left(2\tau-1\right)}{D} \ll 1.$$

and

$$a \sim -\frac{1}{d}, \quad b \sim -\frac{1}{l}, \quad c \sim \frac{1}{d} + \frac{1}{l} = \frac{1}{Kdl},$$

$$\begin{aligned}\sigma_{j\pm} &= c \pm \sqrt{(a+b)^2 - 2abt}, \qquad t = 1-\cos\left(\frac{\pi j}{K}\right) \in (0,2)\\ &= \frac{1}{Kdl} \pm \sqrt{\left(\frac{1}{Kdl}\right)^2 - 2\frac{1}{dl}t}\\ &= \frac{1}{Kdl}\left(1 \pm \sqrt{1-2K^2dlt}\right).\end{aligned}$$

Therefore we obtain

$$\lambda_0 \sim 2ldK\sqrt{\frac{B}{\varepsilon D}}\left(1 - 2\frac{\left(\tau-1\right)\lambda_0+1}{1\pm\sqrt{1-2K^2dlt}}\right).$$

When $\lambda_0 = O\left(1\right)$, the right hand side dominates and we therefore obtain

$$\lambda_0 = \frac{-1\pm\sqrt{1-2K^2dlt}}{2\left(\tau-1\right)}. \tag{3.9}$$

Moreover, since $d = \frac{1}{K} - l$, $l \in \left(0, \frac{1}{K}\right)$, and since $t \in (0,2)$ we see that $2K^2dlt \leq 1$. This shows that in the case $\tau > 1$, the eigenvalues corresponding to the nodes $\sigma_{j\pm}$ are all real negative. The node σ_+ is,

$$\begin{aligned}\sigma_+ &= \mu_d\tanh\left(\mu_d\frac{d}{2}\right) + \mu_l\tanh\left(\mu_l\frac{l}{2}\right)\\ &\sim \mu_d^2\frac{d}{2} + \mu_l^2\frac{l}{2}\\ &\sim \frac{1}{2D}\left(\lambda_0 d + \left(2+\lambda_0\left(2\tau-1\right)\right)l\right),\\ \lambda_0 &\sim 2\sqrt{\frac{B}{\varepsilon D}}\left(ldK - \frac{4D\left[\left(\tau-1\right)\lambda_0+1\right]}{\left(\lambda_0 d + \left(2+\lambda_0\left(2\tau-1\right)\right)l\right)}\right).\end{aligned}$$

Since the third term is asymptotically bigger, the assumption $\lambda_0 = O(1)$ leads to

$$\lambda_0 = \frac{-1}{\tau - 1}.$$

Note that this is a special case of the formula (3.9) with $\pm = -$ and $t = 0$. For the mode σ_- we have

$$\sigma_- = \mu_d \tanh\left(\mu_d \frac{d}{2}\right) + \mu_l \coth\left(\mu_l \frac{l}{2}\right) \sim \frac{2}{l};$$

$$\lambda_0 \sim 2l\sqrt{B\frac{1}{\varepsilon D}}\left(dK - \left[(\tau - 1)\lambda_0 + 1\right]\right),$$
$$\lambda_0 \sim \frac{-1 + Kd}{\tau - 1} \sim \frac{-Kl}{\tau - 1}$$

Note that this is a special case of the formula (3.9) with $\pm = -$ and $t = 2$.

Next we consider large eigenvalues, $\lambda \gg O(\varepsilon)$. Then we have

$$\mu_l \sim \frac{\sqrt{(2\tau - 1)\lambda}}{\sqrt{D\varepsilon}}, \quad \mu_d \sim \frac{\sqrt{\lambda}}{\sqrt{D\varepsilon}},$$

and we write,

$$\lambda \sim 2\sqrt{B}\left(\frac{1}{D}\sqrt{D\varepsilon}ldK - \frac{2}{\left(\sigma/\frac{\sqrt{\lambda}}{\sqrt{D\varepsilon}}\right)}(\tau - 1)\sqrt{\lambda}\right).$$

Dimensional analysis shows that the only way to achieve this balance is when σ is large. But this is only possible when

$$\sinh(\mu_l l) = 0 \quad \text{or} \quad \sinh(\mu_d d) = 0$$

Thus either $\mu_l l = i\pi m$ or $\mu_d d = i\pi m$ where m is some integer. This yields the following eigenvalues,

$$\lambda \sim -D\varepsilon\frac{m^2\pi^2}{l^2(2\tau - 1)} \quad \text{or} \quad \lambda \sim -D\varepsilon\frac{m^2\pi^2}{d^2}.$$

Finally, we show that a Hopf bifurcation occurs in the regime $O(\tau - 1) \ll 1$. Since the small eigenvalues are negative when $\tau - 1 \gg 0$ and positive when $\tau - 1 \ll 0$, the real part changes sign precisely when $O(\tau - 1) \ll 1$. To show that this occurs via a Hopf bifurcation, it suffices to show that λ can never be zero. Suppose not. Then using some algebra we arrive at the following for the modes $\sigma_{j\pm}$

$$-1 \pm \sqrt{1 - 2K^2 dlt} = 0, \quad t = 1 - \cos\left(\frac{\pi j}{K}\right) \in (0, 2)$$

But this is clearly impossible since $K^2 dlt < \frac{1}{4}$ as mentioned above. The modes $\sigma_\pm$ are handled similarly.

This completes the proof of Theorem 2. ■

4 Hopf bifurcation, $DK^2 \ll O\left(\frac{1}{\varepsilon}\ln^2\varepsilon\right)$

As Theorem 2 shows, a Hopf bifurcation occurs when τ is near 1. In this section we study this regime in more detail, culminating in the proof of Theorem 4.

We start by analysing the σ_+ node. We make the assumption that

$$\lambda \ll O(\varepsilon D).$$

This assumption will be verified later on to be consistent with the condition (1.8), $D \gg \sqrt{\frac{B}{\varepsilon D}}$. We have,

$$\mu_l^2 \sim \frac{\lambda + 2\varepsilon}{\varepsilon D} \ll 1, \quad \mu_d \sim \frac{\lambda}{\varepsilon D} \ll 1,$$

and we expand σ_+ up to second order,

$$\begin{aligned}
\sigma_+ &= \mu_d \tanh\left(\mu_d \frac{d}{2}\right) + \mu_l \tanh\left(\mu_l \frac{l}{2}\right) \\
&\sim \frac{\lambda}{\varepsilon D}\frac{d}{2} - \frac{1}{24}\left(\frac{\lambda}{\varepsilon D}\right)^2 d^3 + \frac{\lambda + 2\varepsilon}{\varepsilon D}\frac{l}{2} - \frac{1}{24}\left(\frac{\lambda + 2\varepsilon}{\varepsilon D}\right)^2 l^3 \\
&\sim -\left(\frac{\lambda}{\varepsilon D}\right)^2 \left(\frac{d^3 + l^3}{24}\right) + \frac{\lambda}{\varepsilon D}\left(\frac{1}{2K}\right) + \frac{l}{D}.
\end{aligned}$$

We write the equation for λ as

$$\lambda\sigma \sim 2\sqrt{B\frac{\varepsilon}{D}}\left(ldK\sigma - 2\frac{(\tau - 1)\lambda + \varepsilon}{\varepsilon}\right)$$

or

$$a\lambda^3 + b\lambda^2 + c\lambda + d = 0$$

where

$$\begin{aligned}
a &= \left(\frac{1}{\varepsilon D}\right)^2 \left(\frac{d^3 + l^3}{24}\right), \\
b &= -\frac{1}{\varepsilon D}\left(\frac{1}{2K}\right) - 2\sqrt{B\frac{\varepsilon}{D}}ldK\left(\frac{1}{\varepsilon D}\right)^2 \left(\frac{d^3 + l^3}{24}\right) \\
&\sim -\frac{1}{\varepsilon D}\left(\frac{1}{2K}\right) \quad \text{using (1.8)} \\
c &= -\frac{l}{D} + 2\sqrt{B\frac{\varepsilon}{D}}\left(\frac{ld}{2\varepsilon D} - \frac{2}{\varepsilon}(\tau - 1)\right) \\
&\sim 2\sqrt{B\frac{\varepsilon}{D}}\left(\frac{ld}{2\varepsilon D} - \frac{2}{\varepsilon}(\tau - 1)\right) \\
d &= 2\sqrt{B\frac{\varepsilon}{D}}\left(ldK\left\{\frac{l}{D}\right\} - 2\right) \\
&\sim -4\sqrt{B\frac{\varepsilon}{D}}
\end{aligned}$$

Substituting $\lambda = i\lambda_i$ and separating the real and imaginary part, we find that

$$\lambda_i = \sqrt{\frac{d}{b}}, \quad c = \frac{ad}{b}.$$

This yields,

$$\lambda_i = \sqrt{8K}\left(\varepsilon^3 DB\right)^{1/4}$$

and, keeping also all lower order terms for reference,

$$\tau - 1 \sim \frac{ld}{4D} - \frac{\left(\frac{d^3+l^3}{12}\right)K}{D + \sqrt{B\frac{1}{\varepsilon D}}ldK^2\left(\frac{d^3+l^3}{6}\right)} - \frac{l\varepsilon}{4\sqrt{B\varepsilon D}}. \tag{4.1}$$

The formula (1.9) is obtained by dropping the last term of the right hand side of (4.1) (which is of smaller order than the first term on the right hand side), as well as dropping the second term in the denominator of the second term.

Finally we must also show that the σ_+ mode undergoes a Hopf bifurcation before all other modes. Let us now consider the σ_- mode. We assume here that $\mu_l \sim \frac{\sqrt{\lambda}}{\sqrt{\varepsilon D}} \sim \mu_d$. and we rewrite (3.1) as

$$-4\frac{1}{D}\sqrt{\frac{B}{\varepsilon D}}\left(\tau_0\lambda_0 D + 1\right) = F(\lambda_0) \equiv \lambda_0\sqrt{\lambda_0}\left(\tanh\sqrt{\lambda_0}\frac{d}{2} + \coth\sqrt{\lambda_0}\frac{l}{2}\right)$$

$$\text{where } \tau = 1 + \tau_0, \quad \lambda = \varepsilon D\lambda_0.$$

Near the origin and for real λ_0, the curve $F(\lambda_0) \sim \frac{2}{l}\lambda_0 + \left(\frac{d}{2} + \frac{l}{6}\right)\lambda_0^2$ is convex and increasing. The left hand side is a line in λ_0 and it intersects the y axis at $-\frac{4}{D}\sqrt{\frac{B}{\varepsilon D}}$ which is a very small value by assumption (1.8). Therefore this line will intersect the curve $F(\lambda_0)$ for some small value of λ_0 unless its slope is precisely the slope of $F(\lambda_0)$ at the origin, i.e. $-4\sqrt{\frac{B}{\varepsilon D}}\tau_0 \sim \frac{2}{l}$. This is precisely the scaling on which the Hopf bifurcation occurs. Subsituting $l = \frac{A}{\sqrt{2B}}$ we obtain,

$$\tau_{h_-} \sim 1 - \frac{\sqrt{\varepsilon D}}{\sqrt{2}A}. \tag{4.2}$$

Performing a similar study for the modes $\sigma_{j\pm}$ we obtain

$$\tau_{h_{j\pm}} \sim 1 - \frac{\sqrt{\varepsilon D}}{\sqrt{B}4Kdl}\left(1 \pm \sqrt{1 - 2K^2 dlt}\right), \qquad t = \ t = 1 - \cos\left(\frac{\pi j}{K}\right) \in (0,2). \tag{4.3}$$

But clearly, $\tau_{h_{j\pm}}, \tau_{h_-} < \tau_{h_+}$ since $\frac{\sqrt{\varepsilon D}}{A} \gg O\left(\frac{1}{D}\right)$ by the assumption (1.8). This shows that the eigenvalue λ_+ corresponding to σ_+ undergoes the Hopf bifurcation before any of the other eigenvalues, as τ decreases past τ_{h_+}. ■

In figure 4 we show the Hopf bifurcation values τ_{h_+} and τ_{h_-} computed numerically as well as the asymptotic results (1.9), (4.2), for various values of D while fixing $\delta = \sqrt{D\varepsilon} = 0.01$. This figure shows a very good agreement when $D \gg \delta$.

5 Asymmetric K-mesa solutions and instability with $DK^2 \sim O\left(\frac{1}{\varepsilon}\ln^2\varepsilon\right)$

In Section 3 we have shown that K mesas are always stable provided that $\tau > 1$. In our analysis there, we have ignored the effect of the exponentially decaying tail of v. However as DK^2 increases, this effect eventually must be taken into account. As we will see in this section, this occurs when $D \geq O\left(\frac{1}{\varepsilon\ln^2\varepsilon}\right)$. The main result of this section is the following.

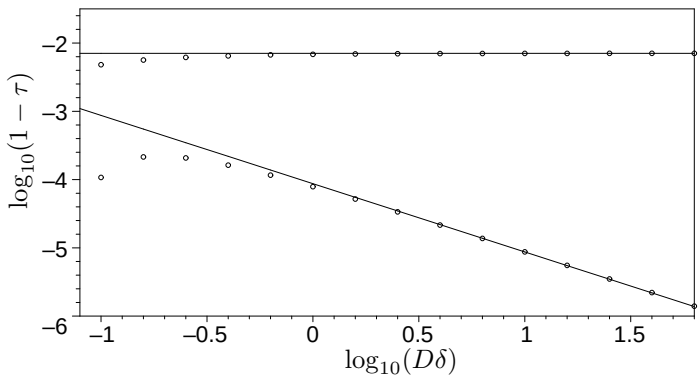

FIGURE 4. The value of τ_{h_+} and τ_{h_-} as a function of D, while $\delta = \sqrt{\varepsilon D} = 0.01$ is held fixed. The dots represent the numerical solution obtained by substituting $\lambda = i\lambda_i$ into (3.1) and solving for τ and λ_i using Newton's method. The solid lines are represent formulas (1.9) and (4.2). Here, $A = 1$ and $B = 15$.

Proposition 8 *Let*

$$f(D) = 3\sqrt{B/2} + \frac{A}{16BD}\left(\sqrt{2B} - A\right)^2 + 3\sqrt{2B}\left(\exp\left\{-\frac{A}{\sqrt{2\varepsilon D}}\right\} + \exp\left\{-\frac{1}{\sqrt{2\varepsilon D}}\left(\sqrt{2B} - A\right)\right\}\right),$$

and let D_1 be the minimum of $f(D)$. Let

$$D_K = \frac{1}{K^2} D_1.$$

Suppose that $\tau > 1$ and $K \geq 2$. Then $K-$ mesa solution of Proposition 1 is stable when $D < D_K$ and unstable when $D > D_K$. The minimum D_1 satisfies the following transcendental equation,

$$\frac{A}{\sqrt{D_1}8B}\left(\sqrt{2B} - A\right)^2 = \frac{3\sqrt{2B}}{\sqrt{2\varepsilon}}\left(A\exp\left\{-\frac{A}{\sqrt{D_1 2\varepsilon}}\right\} + \left(\sqrt{2B} - A\right)\exp\left\{-\frac{1}{\sqrt{D_1 2\varepsilon}}\left(\sqrt{2B} - A\right)\right\}\right). \tag{5.1}$$

Suppose that $2A^2 < B$. Then

$$D_1 \sim \frac{A^2}{2\varepsilon \ln^2\left(\frac{12\sqrt{2}AB^{3/2}}{\varepsilon\left(\sqrt{2B}-A\right)^2}\right)}.$$

Suppose that $2A^2 > B$. Then

$$D_1 \sim \frac{\left(\sqrt{2B} - A\right)^2}{2\varepsilon \ln^2\left(\frac{12\sqrt{2}}{\varepsilon A}B^{3/2}\right)}.$$

Before providing a proof, consider a numerical example. Take

$$\varepsilon = 0.001,\ A = 2,\ B = 18.$$

Then solving (5.1) we obtain $D_1 = 21.16$ so that

$$D_2 = 5.3, \quad D_3 = 2.35.$$

To verify Proposition 8, we ran the full numerical simulation of (1.1) for various values of D. We took $\tau = 3$, the initial condition to be as given in Proposition 1 with $K = 2$, and we took D from 5 to 6 with 0.1 increments every 2500 time units. For each value of D, we then plotted the difference of the height of the two mesas versus time. See Figure 5.a. From this computation, we see that a change of stability occurs when $D \approx 5.5$: if $D < 5.5$ then the difference in height is decreasing but is increasing if $D > 5.5$. This agrees well with the theoretical prediction $D = 5.3$. We then took $K = 3$, and D from 1.9 to 3 with 0.1 increments every 2500 time units. Figure 5.b shows the the difference in heights of the first and second mesa. From this figure we conclude that the change in stability occurs when $D \sim 2.45$. Again, this agrees well with the theoretical prediction of $D_3 = 2.35$.

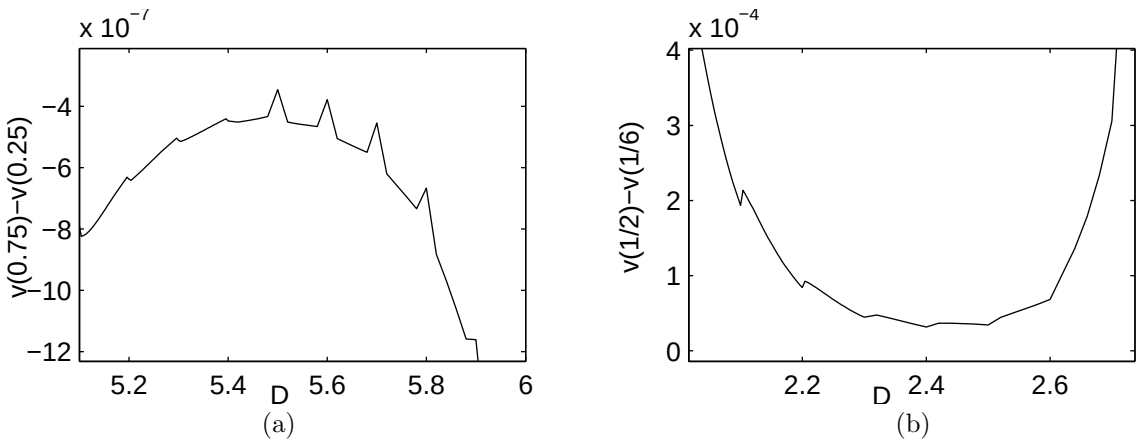

FIGURE 5. (a) The difference in height of a two-mesa solution for various values of D. Here, $D = 5 + 0.1\text{floor}(t/2500)$. Note the change of stability when $D \sim 5.5$. (b) The difference in height of the first two mesas of a three-mesa solution. Here, $D = 1.9 + 0.1\text{floor}(t/2500)$. Note the change of stability when $D \sim 2.45$. In both figures, $\varepsilon = 0.001$, $A = 2$, $B = 18, \tau = 3$.

Proposition 8 follows from the existence of asymmetric patterns. Indeed a similar phenomena was studied for the spike solutions of the Gierer-Meinhardt model [**16**] and in the Gray-Scott model [**19**]. In both of these models, an asymmetric spike pattern was found to bifurcate from a symmetric K spike solution when $K > 1$. Moreover a change of stability of a K-spike pattern occured precisely at that point.

To show existence of asymmetric patterns, it suffices to compute $w(L)$ as a function of the domain length L, and to show an existence of a minimum of this curve. Below we show that such minimum occurs precisely when the the interaction in the u component is balanced by the interaction of v in the exponential tail. The main result is the following.

Lemma 9 *Consider a symmetric mesa-type solution on domain* $[0, L]$. *Then we have,*

$$w(L) \sim 3\sqrt{B/2} + \frac{1}{D}\frac{A}{16B}L^2\left(\sqrt{2B} - A\right)^2 + 3\sqrt{2B}\left(\exp\left\{-\frac{LA}{\sqrt{2\varepsilon D}}\right\} + \exp\left\{-\frac{L}{\sqrt{2\varepsilon D}}\left(\sqrt{2B} - A\right)\right\}\right) \tag{5.2}$$

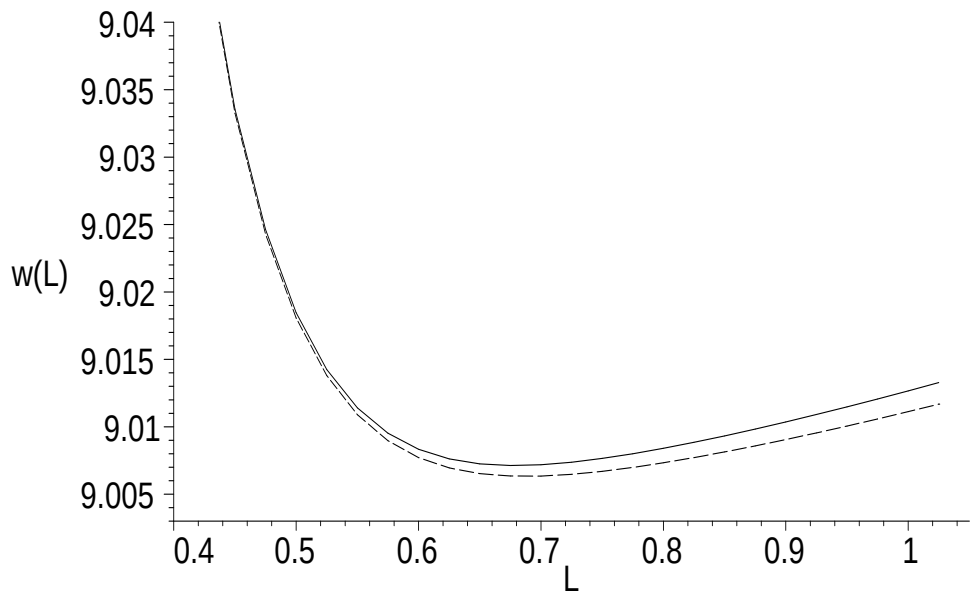

FIGURE 6. The value of $w(L)$ as a function of L. Here, $A = 2,\ B = 18,\ \varepsilon = 0.001$ and $D = 10$. The solid curve represents an exact numerical value computed using the boundary value problem solver; the dashed curve represents the asymptotic formula (5.2). Note that both curves give almost the same minimum value of $L \approx 0.68$

Proof. We recall that upon expanding the solution in $\frac{1}{D}$ as $w = w_0 + \frac{1}{D}w_1 + \ldots$, $v = v_0 + \frac{1}{D}v_1 + \ldots$, the equation for w_1 is

$$\delta^2 v_{1xx} = F_v(v_0, w_0)v_1 + F_w(v_0, w_0)w_1, \tag{5.3}$$

$$w_{1xx} = w_0 - v_0 - A \tag{5.4}$$

Note that we have

$$\delta^2 v'_{0xx} = F_v(v_0, w_0)v'_0.$$

Therefore, upon multiplying (2.8) by v'_0, integrating we obtain,

$$\int_0^{L/2} v'_0 F_w(v_0 w_0)w_1 = \delta^2\left(v_{1x}v_{0x} - v_1 v_{0xx}\right)_{x=0}^{x=L/2}. \tag{5.5}$$

To evaluate the right hand side, we write

$$\int_0^{L/2} v'_0 F_w(v_0 w_0)w_1 \sim w_1(x_l)\int_{x_l^-}^{x_l^+} \frac{d}{dx}G(v_0, w_0)$$

where

$$G(v_0) = \int F_w dv_0 = -Bv_0 + v_0^2 w_0 - \frac{2}{3} v_0^3,$$
$$G(w_0) = \frac{1}{9} w_0^3, \qquad G(\frac{w_0}{3}) = \frac{1}{81} w_0^3.$$

It follows that

$$\int_0^{L/2} v_0' F_w(v_0 w_0) w_1 \sim -w_1\left(x_l\right) \frac{8}{81} w_0^3.$$

To evaluate the right hand side of (5.5) we expand the solution near the boundary.

At $x = 0$, we assumed that $v \sim w_0$; writing

$$v = w_0 + V(x)$$

we then obtain to leading order,

$$\begin{aligned} \delta^2 V'' &= F_v\left(w_0, w_0\right) V + O\left(\frac{1}{D}\right) \\ &\sim BV. \end{aligned}$$

Imposing the boundary condition $V'(0) = 0$ we then obtain

$$V \sim K\left(\exp\left\{-\frac{\sqrt{B}}{\delta} x\right\} + \exp\left\{+\frac{\sqrt{B}}{\delta} x\right\}\right) + O\left(\frac{1}{D}\right)$$

for some constant K. To determine K, we impose the matching condition $w_0 + V \sim v_0 + \frac{1}{D} v_1$ in the region $\frac{\delta}{\sqrt{B}} \ll x \ll x_l$. In this region we obtain

$$\begin{aligned} v_0 &= \frac{2}{3} w - \frac{w}{3} \tanh \frac{x - x_l}{2} \frac{\sqrt{B}}{\delta} \\ &\sim w_0 + \frac{2}{3} w_0 \exp\left\{-\frac{\sqrt{B}}{\delta} x_l\right\} \exp\left\{\frac{\sqrt{B}}{\delta} x\right\}. \end{aligned}$$

Thus we obtain

$$K = \frac{2}{3} w_0 \exp\left\{-\frac{\sqrt{B}}{\delta} x_l\right\}.$$

Moreover, for $x \ll x_l$ we have

$$\delta^2 v_{1xx} \sim B v_1 - B w_1 \tag{5.6}$$
$$\sim B v_1 - B w_1(0) \tag{5.7}$$

so that

$$v_1 \sim w_1\left(0\right) + DK \exp\left\{-\frac{\sqrt{B}}{\delta} x\right\}.$$

It follows that

$$v_{1x}(0)\, v_{0x}(0) \sim \frac{-B}{\delta^2} K^2 D, \qquad v_{1x}(0)\, v_{0xx}(0) \sim \frac{B}{\delta^2}\frac{K^2}{D},$$

$$\delta^2 \left(v_{1x} v_{0x} - v_1 v_{0xx}\right)_{x=0} = -4B^2 D \exp\left\{-\frac{\sqrt{B}}{\delta}(L-l)\right\}.$$

Similarly, near $x = \frac{L}{2}$ we have

$$v_0 \sim \frac{w_0}{3} + \frac{2}{3} w_0 \exp\left\{\frac{-\sqrt{B}}{\delta}\frac{l}{2}\right\} \exp\left\{\frac{-\sqrt{B}}{\delta}\left(x - \frac{L}{2}\right)\right\}$$

from where we deduce

$$v_1 \sim -w_1(0) + D\frac{2}{3} w_0 \exp\left\{\frac{-\sqrt{B}}{\delta}\frac{l}{2}\right\} \exp\left(\frac{\sqrt{B}}{\delta}\left(x - \frac{L}{2}\right)\right),$$

$$\delta^2 \left(v_{1x} v_{0x} - v_1 v_{0xx}\right)_{x=L/2} = -\frac{4B^2}{D} \exp\left\{-\frac{\sqrt{B}}{\delta} l\right\}.$$

Therefore we obtain

$$w_1(x_l)\frac{8}{81} w_0^3 \sim 4B^2 D \left(\exp\left\{-\frac{\sqrt{B}}{\delta} l\right\} + \exp\left\{-\frac{\sqrt{B}}{\delta}(L-l)\right\}\right)$$

$$w_1(x_l) \sim 3\sqrt{2B} D \left(\exp\left\{-\frac{LA}{\sqrt{2}\delta}\right\} + \exp\left\{-\frac{L}{\sqrt{2}\delta}\left(\sqrt{2B} - A\right)\right\}\right).$$

In the region $0 < x < x_l$, we have $v_0 \sim w_0$ so from (2.9), we obtain

$$w_1'' \sim -A, \qquad 0 < x < x_l.$$

It follows that

$$w_1(x_l) - w_1(0) \sim -\frac{A}{2} x_l^2 = -\frac{A}{2}\left(\frac{L-l}{2}\right)^2,$$

Using $w_0 = 3\sqrt{B/2}$, $l = \frac{LA}{\sqrt{2B}}$ we then obtain (5.2). ■

In Figure 6 we compare the asymptotic formula (5.2) with the numerically computed value for $A = 2$, $B = 18$, $\varepsilon = 0.001$ and $D = 10$. Note that the function $L \to w(L)$ has a minimum at $L \approx 0.7$. This shows the existence of a fold point. Now suppose that D is chosen such that this minimum occurs precisely at $L = \frac{1}{K}$, with $K > 1$ an integer. Then the corresponding K-mesa equilibrium solution will have a zero eigenvalue. Since the exponential terms in (5.2) quickly die out as L increases, the solution becomes stable to the right of $L = \frac{1}{K}$, and therefore unstable to the left of it. Proposition 8 is precisely this statement; it is obtained simply by scaling the L out and stating the existence of the fold point in terms of D instead.

6 Turing analysis

In this section we perform a Turing analysis of the homogenous steady state $u = A$, $v = \frac{B}{A}$. In particular, we are interested in examining any possible connections between the

Turing instability regime (which leads to cosinusoidal-like patterns $\cos(2k\pi x)$ of mode k) and the localized mesa-like structures. We start by linearizing (1.1) around the steady state as follows,

$$u = A + \xi e^{\lambda t}\cos(2k\pi x), \quad v = \frac{B}{A} + \eta e^{\lambda t}\cos(2k\pi x), \qquad \xi, \eta \ll 1; \quad 2k \in \mathbb{N}.$$

This yields a 2x2 eigenvalue problem for λ. Its solution is given by

$$\lambda^2 - T\lambda + \Delta = 0,$$

where

$$T = B - \tau A^2 - n(1+\tau) - \varepsilon, \quad \Delta = \tau\left[n\left(n - B + A^2\right) + \varepsilon\left(A^2 + n\right)\right], \qquad n = 4k^2\pi^2\varepsilon D.$$

Note that $\Delta_{n=0} > 0$ so that the zero mode is unstable if $T_{n=0} > 0$ or $B - \tau A^2 > 0$. Numerically, we observe that when the zero mode is unstable, it dominates and the system moves away from the equilibrium and quickly approaches a very long relaxation cycle, before any of the non-zero modes are activated. Therefore no spatial instability is observed. This leads to the following *necessary condition* for the Turing instability to appear:

$$B - \tau A^2 < 0. \tag{6.1}$$

Provided this condition is satisfied, we have $T < 0$ for all n. Therefore Turing instability will occur iff $\Delta < 0$. In particular the second necessary condition is that

$$B - A^2 > 0. \tag{6.2}$$

In this case, the most unstable mode is of the same order as the minimum of Δ,

$$k_*^2 \sim \frac{B - A^2 - \varepsilon}{\pi^2 2\varepsilon D}. \tag{6.3}$$

Shortly after the Turing instability is triggered, localized mesa-type structures appear due to the presence of steep gradients. In this regime, Turing instability cannot predict the final number K of mesas. Indeed, we have $K \le K_*$ where

$$K_* = \max\left(1, \sqrt{\frac{D_1}{D}}\right)$$

with $D_1 = O\left(\frac{1}{\varepsilon \ln^2 \varepsilon}\right)$ as obtained in Theorem 3. It follows that as long as $B - A^2 \gg 0$ and $\tau - 1 \gg 0$, we have

$$K_* = O\left(\frac{1}{\delta \ln \frac{1}{\varepsilon}}\right), \quad k_* = O\left(\frac{1}{\delta}\right), \quad \delta = \sqrt{\varepsilon D}$$

so that $K_* \ll k_*$. Therefore we expect that shortly after the patterns appear, a coarsening process takes place whereby some of the resulting mesas dissapear until there are at most K_* of them left.

Consider an example shown on Figure 1.a. Take $A = 1,\ B = 8,\ \varepsilon = 10^{-4},\ D = 10$. We take $\tau = 10$ to satisfy (6.1). From (5.1) we obtain $D_1 \sim 44.5$ so that $K_* = 2$ and from (6.3) we obtain $k_* = 9$. In a numerical simulation, we started from the homogenous steady state $u = A, v = \frac{B}{A}$, perturbed by a very small random noise. A Turing instability corresponding to the mode $k = 7$ first develops. At time $t \sim 50$ only six modes remain

from which six mesas develop. One by one, these mesas are annihilated until only two remain, confirming our theory. We integrated the system until $t =$ one million, but we do not expect any more mesa refinement since $K_* = 2$.

Formulas (6.3) together with (1.5) show that it is possible for the mesa patterns to be stable even as the homogenous steady state is stable. This occurs when $A^2/2 < B < A^2$ (i.e. $l > \frac{1}{2}$) with $\tau > \frac{B}{A^2}$. A more difficult question is whether one can find a regime in which both are *unstable*, and the system iterates between the two. Here we consider the case where D satisfies (1.8). In this regime the instability of a single mesa solution can only occur when τ is near 1. Then (6.1) and (6.2) together imply that $A \sim B^2$. So we set:

$$B = A^2 + \alpha, \quad \alpha \ll 1.$$

From the condition $T_{n=0} \leq 0$ we obtain

$$\tau \geq 1 + \frac{\alpha - \varepsilon}{A^2}$$

and we and suppose that a single mode $k = 1 \implies n = n_* = 4\pi^2 \varepsilon D$ is unstable. The condition $\Delta_{n=n_*} < 0$ then leads, to leading order:

$$4\pi^2 \varepsilon D \left(\varepsilon D 4\pi^2 - \alpha\right) + \varepsilon A^2 < 0$$

so that to leading order,

$$\alpha \geq \frac{A^2}{D 4\pi^2} + 4\pi^2 \varepsilon D$$

from where

$$\tau \geq 1 + \frac{1}{D 4\pi^2} \sim 1 + 0.025 \frac{1}{D}.$$

On the other hand, we have $B \sim A^2 \implies l = \frac{1}{\sqrt{2}}$; and we have

$$ld - \frac{l^3 + d^3}{3} = 2l - 2l^2 - \frac{1}{3} = \sqrt{2} - 1 - \frac{1}{3}$$

so that from Theorem 4 we obtain

$$\tau_h \sim 1 + 0.020 \frac{1}{D}.$$

Therefore the instability of a mesa cannot follow the Turing instability since $\tau > \tau_h$.

7 Discussion

In Section 5 we were able to determine the instability thresholds without actually computing the eigenvalues; but simply by showing the existence of an asymmetric pattern bifurcating from a fold point. It is an open problem to find the full expression for the eigenvalues near this threshold. This would give a theoretical timescale for each of the step in the coarsening process. We expect that the unstable eigenvalue will decrease exponentially in the distance between the mesas. This would explain the exponential time increase between the successive coarsening events, as observed in Figure 1.a

In Theorem 4 under condition (1.8) we have shown that as τ is decreased near 1, the first eigenvalue to cross the imaginary axis is λ_+, whose eigenfunction is even. This

corresponds to a "breather"-type instability shown on Figure 1.b. An open question is whether there exists a regime for which other eigenvalues undergo a Hopf bifurcation before the λ_+ eigenvalue. For the Gray-Scott model it is known that a single spike can undergo a Hopf bifurcation due to a slow translational instability – which corresponds to an odd eigenfunction – whereby the center of the spike oscillates periodically [**19**], [**10**], [**20**]. The analogy of this phenomenon for a single mesa of the Brusselator would be the Hopf bifurcation of the λ_- eigenvalue. One can also imagine spike-type solutions for the Brusselator simply by taking the limit $l \to 0$ or equivalently, $B \to \infty$. It is an open problem to study this regime.

It would be interesting to study the slow dynamics of the mesas, of which there are several types, corresponding to different eigenvalues. The first type is the slow translational motion of the mesa such as seen in Figure 3 after time $t \sim 2200$. Similar motion has been analysed for the FitzHugh-Nagumo model on an infinite line [**15**]. In contrast to the Brusselator however, the FitzHugh-Nagumo model does not have a mass conservation constraint $lK \sim \frac{A}{\sqrt{2B}}$ derived in Proposition 1, and does not undergo a coarsening process. In this sense the Brusselator resembles more the Cahn-Hilliard model or the Allen-Cahn model with mass constraint [**32**], [**34**]. However unlike the Cahn-Hilliard model, the Brusselator does not have a variational formulation, and the mass conservation is only asymptotically valid. We remark that a similar phenomenon was also studied for Gray Scott and Gierer-Meinhardt models in the context of spike solutions [**16**], [**9**], [**21**].

A second type of slow instability is the mass exchange that occurs prior to mesa annhiliation as seen in Figure 3 at time $t \sim 2000$. This phenomenon also occurs in some flame-propagation problems [**5**], [**33**] and in the Keller-Segel model [**17**], where an exchange of mass takes place between two boundary spikes, and eventually leads to an annihilation of one of them.

The coarsening process in the brusselator terminates when there are $K = O\left(\frac{1}{\delta \ln \varepsilon^{-1}}\right)$ mesas left, where δ is the characteristic width of the interface. This is in contrast to the the Cahn-Hilliard model, where the coarsening proceeds until all but one interface remains [**32**].

Localized structures far from the Turing regime are commonplace in reaction-diffusion systems such as the Brusselator, and provide an alternative pattern-formation mechanism to Turing instability. These structures appear whenever the Turing instability band is very large or when the diffusivity ratio of the activator and inhibitor is large. As we demonstrate in this work, Turing analysis cannot explain the diverse phenomena that can occur in this regime, such as coarsening and the "breather"-type instabilities. However singular perturbation tools can be successfully applied to asnwer many of these questions.

8 Appendix A: proof of Lemma 7

Proof. Note that (3.6) is equivalent to solving

$$\begin{gathered} u'' - \mu_l^2 u = 0, \quad x \in \cup (x_{li}, x_{ri}) \\ u'' - \mu_d^2 u = 0, \quad x \notin \cup (x_{li}, x_{ri}) \\ u'\left(x_{li}^+\right) - u'\left(x_{li}^-\right) = -b_{li}, \qquad u'\left(x_{ri}^+\right) - u'\left(x_{ri}^-\right) = -b_{ri}, \\ u'(0) = 0 = u'(1). \end{gathered}$$

When $x \in [x_{li,} x_{ir}]$ we have

$$u = u_{li} \cosh\left(\mu_2 \left(x - x_{li}\right)\right) + B_{li} \sinh\left(\mu_2 \left(x - x_{li}\right)\right), \quad x \in [x_{li,} x_{ir}], \quad i = 1 \ldots K$$

where $u_{li} = u\left(x_{li}\right)$ and B_{li} is to be found. We similarly have

$$u = u_{ir} \cosh\left(\mu_1 \left(x - x_{ri}\right)\right) + B_{di} \sinh\left(\mu_1 \left(x - x_{ri}\right)\right), \quad x \in \left[x_{ri,} x_{l(i+1)}\right], \quad i = 1 \ldots K - 1.$$

We define

$$d \equiv x_{r(i+1)} - x_{li} = \frac{1 - l}{K},$$

$$\begin{gathered} c_1 \equiv \cosh\left(\mu_l l\right), \quad s_1 \equiv \cosh\left(\mu_l l\right) \\ c_2 \equiv \cosh\left(\mu_d d\right), \quad s_2 \equiv \cosh\left(\mu_d d\right). \end{gathered}$$

We have $u_{ri} = u_{li} c_l + B_{li} s_l$ from where

$$B_{li} = \frac{u_{ri} - u_{li} c_l}{s_l}, \quad i = 1 \ldots K$$

and similarly $u_{l(i+1)} = u_{ir} c_d + B_{ri} s_d$ so that

$$B_{di} = \frac{u_{l(i+1)} - u_{ri} c_d}{s_d}, \quad i = 1 \ldots K - 1$$

We also have

$$\begin{aligned} b_{li} &= u'\left(x_{li}^-\right) - u'\left(x_{li}^+\right) = \mu_d \left(u_{r(i-1)} s_d + B_{d(i-1)} c_d\right) - \mu_l B_{li} \\ &= \mu_d \left(u_{r(i-1)} s_d + \frac{u_{li} - u_{r(i-1)} c_d}{s_d} c_d\right) - \mu_l \frac{u_{ri} - u_{li} c_l}{s_l} \\ &= -\frac{1}{s_d} \mu_d u_{r(i-1)} + \left(\frac{c_d}{s_d} \mu_d + \frac{c_l}{s_l} \mu_l\right) u_{li} - \frac{1}{s_l} \mu_l u_{ri}, \qquad i = 2 \ldots K \end{aligned}$$

and similarly

$$b_{ri} = -\frac{1}{s_l} \mu_l u_{li} + \left(\frac{c_d}{s_d} \mu_d + \frac{c_l}{s_l} \mu_l\right) u_{ri} - \frac{1}{s_d} \mu_d u_{r(i+1)}, \qquad i = 1 \ldots K - 1.$$

Next note that

$$u = A \cosh\left(\mu x\right), \quad x \in [0, x_{l1}]$$

for some constant A. Matching $u\left(x_{l1}^{-}\right)=u\left(x_{l1}^{+}\right)$ we then obtain

$$u=\frac{u\left(x_{l1}\right)}{c_{d/2}}\cosh\left(\mu x\right),$$
$$u'\left(x_{l1}^{-}\right)=u\left(x_{l1}\right)\mu\frac{s_{d/2}}{c_{d/2}}.$$

where $s_{d/2}\equiv\sinh\left(\mu_d d/2\right)$, $c_{d/2}\equiv\cosh\left(\mu_d d/2\right)$. Next we use the following identity,

$$\frac{\sinh\left(x/2\right)}{\cosh(x/2)}=\frac{\cosh\left(x\right)-1}{\sinh(x)}=\frac{\sinh(x)}{1+\cosh(x)}$$

to obtain

$$u'\left(x_{l1}^{-}\right)=\mu\frac{c_d-1}{s_d}u\left(x_{l1}\right).$$

Therefore we obtain

$$\begin{aligned}b_{l1}&=\mu\frac{c_d-1}{s_d}u_{l1}-u'\left(x_{li}^{+}\right)\\&=\mu\frac{c_d-1}{s_d}u_{l1}-\mu\frac{u_{r1}-u_{l1}c_l}{s_l}\\&=\mu\left(\frac{-1}{s_d}\mu_d+\frac{c_d}{s_d}\mu_d+\frac{c_l}{s_l}\mu_l\right)u_{l1}-\frac{1}{s_l}\mu u_{r1}\end{aligned}$$

and similarly

$$b_{rK}=-\frac{1}{s_l}\mu_l u_{lK}+\left(\frac{-1}{s_l}\mu_l+\frac{c_d}{s_d}\mu_d+\frac{c_l}{s_l}\mu_l\right)u_{lK}.$$

This yields the matrix $\mathbf{M}$:

$$\mathbf{M}=\begin{bmatrix}a+c & b & & & & & \\ b & c & a & & & & \\ & a & c & b & & & \\ & & & \cdots & & & \\ & & & & a & c & b \\ & & & & & b & c+a\end{bmatrix}$$

where

$$a=\frac{-\mu_d}{s_d},\qquad b=\frac{-\mu_l}{s_l},\qquad c=\frac{c_d}{s_d}\mu_d+\frac{c_l}{s_l}\mu_l.$$

Consider the matrix

$$Q=\begin{bmatrix}a & b & & & & & \\ b & 0 & a & & & & \\ & a & 0 & b & & & \\ & & & \cdots & & & \\ & & & & b & 0 & a \\ & & & & & a & 0 & b \\ & & & & & & b & a\end{bmatrix}.$$

The eigenvalues of this matrix were computed in [**29**] (see Appendix B). It was found

that Q has the following eigenvalues,

$$\pm\sqrt{a^2+b^2+2ab\cos(\theta)}, \quad \theta=\frac{\pi j}{K}, \quad j=1\ldots K-1$$
$$a+b, \qquad a-b.$$

But we have $M=(Q+c)$. Therefore the eigenvalues of M are given by

$$\left(c\pm\sqrt{a^2+b^2+2ab\cos(\theta)}\right), \quad \theta=\frac{\pi j}{K}, \quad j=1\ldots K-1$$
$$c+a+b, \quad c+a-b.$$

References

[1] N. D. Alikakos, X. Chen, G. Fusco, *Motion of a Droplet by Surface Tension Along the Boundary*, Calc. Var. Partial Differential Equations, 11, No. 3, (2000), pp. 233-305.

[2] N. D. Alikakos, G. Fusco, C. Stephanopolous, *Critical Spectrum and Stability of Interfaces for a Class of Reaction-Diffusion Equations*, J. Differential Equations, 126, No. 1, (1996), pp. 106-167.

[3] J.F.G. Auchmuty and G. Nicolis, *Bifurcation analysis of nonlinear reaction-diffusion equations - I. Evolution equations and the steady state solutions*, Bull. Math. Biol. 37, 323-365 (1975).

[4] J. Bard and I. Lauder, *How well does Turing's theory of morphogensis work?*, J. Theor. Biol. 45, 501-531 (1974)

[5] H. Berestycki, S. Kamin and G. Sivashinsky, *Nonlinear dynamics and metastability in a Burgers type equation*, Compte Rendus Acad. Sci., Paris 321(1995), 185-190.

[6] X. Chen, Spectrum for the Allen-Cahn, Cahn-Hilliard, and Phase-Field Equations for Generic Interfaces, Comm. Partial Differential Equations, 19, No. 7-8, (1994), pp. 1371-1395.

[7] A. Cornish-Bowden, *Fundamentals of Enzyme Kinetics (3rd edition)*, Portland Press, London, 2004

[8] A. Doelman and D. Iron, *Destabilization of fronts in a class of bistable systems*, Physica D, 35(6), 1420-1450.

[9] A. Doelman, W. Eckhaus, T. J. Kaper, *Slowly Modulated Two-Pulse Solutions in the Gray-Scott Model I: Asymptotic Construction and Stability*, SIAM J. Appl. Math., **61**, No. 3, (2000), pp. 1080-1102.

[10] A. Doelman, R. A. Gardner and T. J. Kaper, *Stability Analysis of Singular Patterns in the 1D Gray-Scott Model: A Matched Asymptotics Approach*, Physica D, 122, No. 1-4, (1998), pp. 1-36.

[11] T. Erneux, J. Hiernaux and G. Nicolis, *Turing's theory in morphogenesis*, Bull. Math. Biol. 40, 771-789 (1978)

[12] T. Erneux and E. Reiss, *Brusselator isolas*, SAIM J. Appl. Math. 43, 1983, 1240-1246.

[13] Paul C. Fife, personal communications.

[14] Jarah Elsvin, personal communications.

[15] R.E. Goldstein, D.J. Muraki and D.M. Petrich, *Interface proliferation and the growth of labyrinths in a reaction-diffusion system*, Phys. Rev. E, Vol 53(4), 1996, 3933-3957.

[16] D. Iron, M. J. Ward, J. Wei, *The Stability of Spike Solutions to the One-Dimensional Gierer-Meinhardt face Model*, Physica D, 150, No. 1-2, (2001), pp. 25-62.

[17] K. Kang, T. Koloklnikov and M.J. Ward, *Spike stability and dynamics in the one dimensional Keller-Segel model*, in preparation.

[18] H. Kidachi, *On Mode Interactions in Reaction Diffusion Equation with Nearly Degenerate Bifurcations*, Progress of Theoretical Physics, Vol. 63, No. 4, April 190, 1152-1169.

[19] T. Kolokolnikov, M. Ward and J. Wei, *Slow Translational Instabilities of Spike Patterns in the One-Dimensional Gray-Scott Model*, submitted, Interfaces and Free Boundaries, (2005), 39 pages.

[20] C. Muratov and V. V. Osipov, *Stability of the Static Spike Autosolitons in the Gray-Scott Model,* SIAM 1-205. J. Appl. Math., 62, No. 5, (2002), pp. 1463-1487.

[21] C.B. Muratov, V.V. Osipov, *Static spike autosolitons in the Gray-Scott model*, J. Phys. A 33 (2000), 8893-8916.

[22] G. Nicolis and I. Prigogine, *Self-Organization in Nonequilibrium Systems*, Wiley, New York, 1977.

[23] Y.Nishiura. *Coexistence of infinitely many stable solutions to reaction-diffusion system in the singular limit*, in Dynamics Reported: Expositions in Dynamical Systems, Edited by C.R.K.T. Jones, U. Kirchgraber and H.O. Walther, volume 3. Springer-Verlag, New York, 1994.

[24] Y. Nishiura, H. Fujii, *Stability of Singularly Perturbed Solutions to Systems of Reaction-Diffusion Equations*, SIAM J. Math. Anal., 18, (1987), pp. 1726-1770.

[25] Y. Nishiura, H. Fujii, *SLEP Method to the Stability of Singularly Perturbed Solutions with Multiple Internal Transition Layers in Reaction-Diffusion Systems*, in Dynamics of Infinite-Dimensional Systems (Lisbon, 1986), pp. 211-230, NATO Adv. Sci. Inst. Ser. F Comput. Systems Sci, 37, Springer, Berlin (1987).

[26] Y. Nishiura, M. Mimura, H. Ikeda, H. Fujii, *Singular Limit Analysis of Stability of Traveling Wave Solutions in Bistable Reaction-Diffusion Systems*, SIAM J. Math. Anal., 21, (1990), pp. 85-122.

[27] Y. Nishiura and M. Taniguchi, *Stability and characteristic wavelength of planar interfaces in the large diffusion limit of the inhibitor*, Proc. Roy. Soc. Edinburgh Sect. A 126 (1996), no. 1, 117-145.

[28] I. Prigogine and R. Lefever, *Symmetry-breaking instabilities in dissipative systems*, J. Chem. Phys. 48, 1965-1700 (1968)

[29] X. Ren and J. Wei, *On the spectra of 3-D lamellar solutions of the Diblock Copolymer problem,* SIAM J. Math. Anal. 35(1)(2003), 1-32.

[30] B. Peña and C. Pérez-García, *Stability of Turing patterns in the Brusselator model*, Phys. Rev. E. Vol. 64(5), 2001.

[31] A.M. Turing, *The chemical basis of morphogenesis*, Phil. Trans. R. Soc., London B237, 37-72 (1952)

[32] L. Reyna, and M.J. Ward, *Metastable Internal Layer Dynamics for the Viscous Cahn-Hilliard Equation*, Methods and Applications of Analysis Vol. 2 (1995), pp. 285-306.

[33] X. Sun and M.J. Ward, *Metastability for a Generalized Burgers Equation with Applications to Propagating Flame–Fronts*, European J. Appl. Math. 10, (1999), 27-53

[34] M.J. Ward, *Metastable Bubble Solutions for the Allen-Cahn Equation with Mass Conservation* SIAM J. Appl. Math. Vol. 56, No. 5, (1996), pp. 1247-1279.

[35] A. De Wit, *Spatial Patterns and Spatiotemporal Dynamics in Chemical Systems*, Advances in Chemical Physics, 109. I. Prigogine and S.A. Rice, editors.

[36] A. De Wit, P. Borckmans and G. Dewel *Twist grain boundaries in three-dimensional lamellar Turing structures*, Proc. Natl. Acad. Sci. USA, Vol 94, 1997, pp. 12765-12768.

[37] A. De Wit, D. Lima, G. Dewel and P. Borckmans, *Spatiotemporal dynamics near a codimension-two point*, Phys. Rev. E. Vol 54(1), 1996